

Soil moisture response to snowmelt and rainfall in a Sierra Nevada mixed-conifer forest

Roger C. Bales, Sierra Nevada Research Institute, UC Merced^a

Jan W. Hopmans, Dept., Land, Air and Water Resources, UC Davis

Anthony T. O'Geen, Dept. Land, Air and Water Resources, UC Davis

Matthew Meadows, Sierra Nevada Research Institute, UC Merced

Peter C. Hartsough, Dept. Land, Air and Water Resources, UC Davis

Peter Kirchner, Sierra Nevada Research Institute, UC Merced

Carolyn T. Hunsaker, USFS Pacific Southwest Research Station, Fresno, CA

Dylan Beaudette, Soils and Biogeochemistry Graduate Group, UC Davis

^aContact information for corresponding author:

Roger C. Bales
Sierra Nevada Research Institute
University of California, Merced
5200 N. Lake Rd.
Merced, CA 95343
209-228-4348 (o)
209-228-4047 (fax)
rbales@ucmerced.edu

Manuscript submitted for Special issue of Vadose Zone Journal

January 5, 2011

Abstract

Co-located, continuous snow-depth and soil-moisture measurements were deployed at two elevations in the rain-snow transition region of a mixed-conifer forest in the Southern Sierra Nevada. At each elevation sensors were placed in the open, under the canopy, and at the drip edge on both north- and south-facing slopes. Snow sensors were placed at 27 locations, with soil moisture and temperature sensors placed at depths of 10, 30, 60 and 90 cm beneath the snow sensor; in some locations depth of placement was limited by boulders or bedrock. Soils are weakly developed (Inceptisols and Entisols) formed from decomposed granite with properties that change with elevation. The soil-bedrock interface is hard in upper reaches of the basin (> 2000 m) where glaciers have scoured the parent material approximately 18,000 yrs ago. Below an elevation of 2000 m soils have a paralithic contact (weathered saprolite) that can extend beyond a depth of 1.5-m facilitating pathways for deep percolation. Soils are wet and not frozen in winter, and dry out in weeks following spring snowmelt and rain. Based on data from two snowmelt seasons, it was found that soils dry out following snowmelt at relatively uniform rates; however the timing of drying at a given site may be offset by up to four weeks owing to heterogeneity in snowmelt at different elevations and aspects. Spring and summer rainfall mainly affected sites in the open, with drying after a rain event being faster than following snowmelt. The drying responses of soil moisture at depths of 30 and 60 cm were similar and generally systematic; with drying responses at 10 cm affected by the groundcover and litter layer. Responses at both 60 and 90 cm showed evidence of low-porosity saprolite and short circuiting at some locations. Water loss rates of 0.5-1.0 cm d⁻¹ during the winter and snowmelt season reflect a combination of evapotranspiration and deep drainage, as stream baseflow remain relatively low. We speculate that much of the deep drainage is stored locally in the deeper regolith during period of high precipitation, being available for tree transpiration during summer and fall months when shallow soil-water storage is limiting. Total annual evapotranspiration for water year 2009 was estimated to be approximately 93 cm.

Introduction

Soil moisture is a fundamental property of mountain forests, with patterns of soil moisture linked to climate, soil properties, plant water use, streamflow, forest health, and other ecosystem features. Intuitively, soil moisture and water flux through forest soils are linked to rain and snowmelt patterns, soil-drainage properties, and withdrawal of water from the soil by plants and evaporation (Robinson et al. 2008). The link between snowmelt and soil moisture at the catchment-scale is important for improving hydrologic predictions and amenable to study using low-cost advances in sensor technology (Bales et al. 2006; Vereecken et al. 2008).

The mixed-conifer zone in the forests of California's Sierra Nevada is a productive ecosystem, with tree heights exceeding 50 m and forest densities, or canopy closures, exceeding 80% in places. Average 50-year precipitation recorded at rain gages in the southern Sierra Nevada is about 100 cm (<http://cdec.water.ca.gov/>), and is a mix of rain and snow. This productive ecosystem lies in that rain-snow transition zone, receiving mainly rain at the lower elevations (~1500 m) and mainly snow above ~2200 m. In contrast to higher elevations it is sufficiently warm to allow tree growth much of the year, and has sufficient moisture to avoid the summer shutdown of growth that occurs at lower elevations. However, this transition zone is sensitive to long-term shifts in temperature, and thus to the fraction of rain versus snow, timing of snowmelt, and seasonal patterns of water use (van Mantgem et al. 2006; Christensen et al. 2008). We currently lack the predictive ability for the bi-directional influences of snow distribution and melt, soil moisture, and vegetation that is necessary to address the impacts of changes in forest properties and climate variables on the forest water cycle. This predictive ability is needed to support decisions involving forest thinning and vegetation management, water use for hydropower, in-stream benefits and downstream water supply, and other ecosystem services. Soil moisture is a sensitive variable, whose spatial patterns control catchment-scale water fluxes (Band 1993).

While there have been advances in determining the variables controlling snow distribution and melt in mountain forests, thus providing a basis for measurement design, similar advances in soil-moisture measurement are lacking (Rice and Bales 2010). Prior results from snow surveys show that differences in snow depth depend on elevation, aspect, slope and canopy cover (Molotch and Bales 2005). In two mixed conifer forests in Colorado and New Mexico, it was observed that in a year with heavy snowfall three sensors placed in the open had up to 50%

greater peak snow depth and longer snow persistence than three paired sensors placed under the canopy, with differences observed in wet but not dry years (Molotch et al. 2009). A prior report for the New Mexico site also noted that ablation rates were generally greater in open areas (Musselman et al., 2008). As has been noted in studies in the boreal forest, the inverse correlation of daily melt rates with snow water equivalent in denser stands results in more-rapid depletion of snow-covered area than in stands with more-uniform snowcover and thus melt rates (Faria et al. 2000). This heterogeneity will have a major influence on meltwater delivery to the soil and deeper regolith, and potentially to available soil moisture.

The aims of the research reported here at the scale of a headwater catchment in mixed-conifer forest were: i) to determine how the response of soil moisture to snowmelt and rainfall is controlled by variability across the landscape, as determined by terrain attributes and soil properties, and ii) to establish how these responses both reflect and constrain other components of the catchment-scale water balance.

Methods

Research involved a measurement program to characterize soils and to continuously monitor snow, precipitation, soil moisture, streamflow, temperatures, and energy balance in a headwater catchment. Results of those measurements were analyzed to provide estimates of stores and fluxes of water over two water years (October 1, 2007 to September 30, 2009).

Location and setting. The study was carried out in the Southern Sierra Critical Zone Observatory (CZO) (37.068°N, 119.191°W), which is co-located with the Kings River Experimental Watersheds (KREW), a catchment-scale, integrated ecosystem project for long-term research on nested headwater streams in the Southern Sierra Nevada (Figure 1). KREW is operated by the U.S. Forest Service, Pacific Southwest Research Station, which is part of the research and development branch of the U.S. Forest Service, under a long-term (50-year) partnership with the Forest Service's Pacific Southwest Region. KREW has been a watershed research site since 2001. The 2.8 km² CZO basin includes three sub-catchments with areas of 49 (P304), 99 (P301), and 132 ha (P303). Most of the reported measurements were conducted in or below P303, at the upper and lower meteorological (met) station sensor-cluster sites. Selected data will be presented for the Critical Zone Tree (CZT-1) location in P301, including soil

moisture and soil physical data. CZT-1 is situated along a ridge in a relatively open area of the forest at an elevation of 2018 m.

The CZO is largely in Sierran mixed-conifer forest (76 to 99%), with some mixed chaparral and barren land cover. Sierran mixed-conifer vegetation in this location consists largely of white fir (*Abies concolor*, ac), ponderosa pine (*Pinus ponderosa*, pp), Jeffrey pine (*Pinus Jeffrey*), black oak (*Quercus kelloggii*, qk), sugar pine (*Pinus lambertiana*, pl) and incense cedar (*Calocedrus decurrens*, cd). These abbreviations are used in selected figures (no Jeffrey pine instrumented).

The soil parent material is colluvium and residuum derived from granite, granodiorite, and quartz diorite, with the Shaver and Gerle-Cagwin soil families dominating the basin (Giger and Schmitt, 1993). The dominant aspect is southwest.

Each of the streams draining the three perennial sub-catchments has two Parshall-Montana flumes, one for measuring high flows and a smaller one for moderate and lower flows. The two KREW met stations are located at elevations of 1750 and 1984 m. Methods for stream and meteorological measurements were described previously (Hunsaker et al. (in review)).

Soil-moisture and snow-depth observations. Snow-depth, soil-moisture and temperature sensors were deployed in 2007 at five locations in the vicinity of the two met stations (Figures 1b and 1c). These sensors are part of a prototype water-balance instrument cluster that includes an eddy-covariance flux tower and additional sensor nodes deployed in 2008-2009 (Bales et al. 2011 (in press)). At both the upper and lower met stations measurement nodes were sited on north- and south-facing aspects; additional nodes were located on flat ground near the upper met station. The following abbreviations are used in subsequent figures to identify sensor locations at the upper and lower met stations: upper south (US), upper north (UN), upper flat (UF), lower south (LS), lower north (LN). Within each location at least two trees were selected, and sensors placed under the canopy (uc) and at the drip edge (de) of both. A third tree was instrumented at UN, for a total of 11 trees. Sensors were also placed in the open (op) at each of the five locations. Combining this notation, UNcd-de indicates the node located near the upper met station (U), north-facing aspect (N), at the drip edge (de) of an incense-cedar (cd).

The five locations, or groups of nodes, had ground slopes ranging from 7 to 18°. At each node an ultrasonic snow depth sensor (Judd Communications) was mounted on a steel arm extending about 75 cm from a vertical steel pipe that was anchored to a u-channel driven into the

ground (seven snow-depth sensors at UN). Snow-depth sensors were mounted 3 m above the ground, with extensions available if needed. One-meter deep 30-cm diameter soil profiles were excavated beneath each snow sensor, and instrumented with soil-temperature and volumetric-water-content sensors (Decagon ECH₂O-TM) placed horizontally at depths of 10, 30, 60 and 90 cm. Excavated profiles were backfilled and hand compacted to maintain the same horizons and density insofar as possible. Depths were measured from the soil surface, and include litter layers in some cases. In total 27 snow sensors and 105 soil-moisture sensors were deployed across the 27 nodes. At three vertical profiles it was not possible to reach a depth of 90 cm owing to boulders or bedrock. Raw data from this embedded-sensor network were archived in our digital library (<https://snri.ucmerced.edu/CZO>), formatted, calibrated and gaps filled by interpolation or correlation with other sensors before analysis.

In August 2008, the soil surrounding a white fir tree (CZT-1) in P301 was instrumented with soil moisture, temperature, electrical conductivity (Decagon 5TE), and matric potential (Decagon MPS-1) sensors. Reported data were collected from six vertical soil profiles within a 5-m radius from the tree trunk, each containing four MPS-1 and four 5TE sensors inserted at depths of 15, 30, 60 and 90 cm into the soil. Three sap-flow sensors (TransfloNZ) were installed in the trunk of CZT-1, with sap flow estimated using the compensation-heat-pulse technique (Green and Clothier 1988).

The soil-moisture sensors installed for this study, the ECH₂O-TM and 5TE (5.2 cm probe length), are successors to the family of Decagon ECH₂O sensors studied by Kizito et al. (2008). That study evaluated the EC-5 and ECH₂O-TE sensors for a wide range of soil-solution salinity and temperature and various soil types. Their calibration measurements showed little probe-to-probe variability, and demonstrated that a single calibration curve was sufficient for a range of mineral soils, suggesting there is no need for a soil-specific calibration. This study concluded that the volumetric water content (VWC) error was reduced to about 0.02 VWC, with a low sensitivity to confounding soil environmental factors such as temperature and soil-solution salinity. Laboratory calibration using the same soil types as did Kizito et al. (2008), including disturbed soil samples from near the CZT-1 location, showed an uncertainty of about 0.05 VWC that was largely the result of an offset near zero soil moisture, resulting in negative VWC values in the dry range. After correction of the sensor output data by using the Topp et al. (1980) calibration curve, the offset in the calibration was eliminated, while maintaining accurate water-

content values in the wet soil-moisture range, resulting in an expected accuracy of about ± 0.02 VWC for laboratory conditions. However, we would expect higher uncertainty of VWC for the field-installed moisture sensors. VWC values across the monitoring depths were converted to total soil water storage values for 75- and 100-cm soil depths.

Soil measurements. At the time of excavation representative soil samples were collected from each location and depth that a soil-moisture sensor was placed. Samples were analyzed for particle size and gravel content. Litter depth, root characteristics, and the presence and size of macropores were noted for each depth. In addition, 16 separate undisturbed soil samples were collected in four soil profiles at the same depths around CZT-1 for measurement of soil bulk density and saturated hydraulic conductivity.

In the laboratory soil samples were air dried and sieved with a 2-mm sieve; all material >2 mm was reported as rock fraction (gravel) by mass. The remaining fine-earth fraction was analyzed for particle size using the pipette method (Gee and Or 2002) and reported as USDA size fractions, very-coarse sand (1-2 mm), coarse sand (0.5-1 mm), medium sand (0.25-0.5 mm), fine sand (0.1-0.25 mm), very-fine sand (0.05-0.1 mm), silt, and clay. Saturated hydraulic conductivity, K_s , was measured by the constant-head method (Reynolds and Elrick 2002).

A soil-depth model was built from 234 soil-depth observations, collected along a grid within the basin to a maximum of 100 cm. Fifty of the points were determined by manual excavation and 193 by depth of penetration using a metal rod. The model was fit using multiple linear regressions with predictor variables selected according to parameters that typically affect or are affected by soil depth: surface slope, tree location, and vegetation density. The soils in this region are strongly influenced by erosion and colluvial processes, with shallower soils found along steeper slopes and deeper soils found at less-steep gradients. Tree location and vegetation density in this region are partially controlled by soil-water-holding capacity, which is largely a function of soil depth at the study site. Vegetation density was also used as proxy for identifying large rock outcrops, where the surrounding soil is likely to be shallow. Predictor variables were extracted from a digital-elevation model (DEM) and 2009 National Aerial Imagery Project (NAIP) imagery. Slope angle was computed from USGS 10-m resolution DEM data, obtained from <http://ned.usgs.gov> (accessed 2010-06-01) (Gesch et al., 2009). Tree location and vegetation density were approximated with the Normalized Difference Vegetation Index (NDVI), calculated from four-band NAIP imagery (red, green, blue, near infra-red), and the first

two principal components of the same NAIP image. The expected non-linear relationship between soil depth and slope angle was accommodated by adding three basis functions (of slope) using restricted cubic splines (RCS) with three knots (Harrell 2001). Predictions were truncated to the original range of the soil-depth measurements (0-100 cm), and smoothed with a 5×5-cell mean filter.

Water balance. Monthly, quarterly, and annual water balances were computed for the shallow (<1 m) and deep (>1 m) soil compartments of P301 and P303:

$$\Delta S_S = Rain + Snowmelt - ET_S - Deep_drainage \quad [1a]$$

and

$$\Delta S_D = Deep_drainage - ET_D - Streamflow \quad [1b]$$

where ΔS_S and ΔS_D are changes in storage for the shallow and deeper soil, respectively; ET_S and ET_D represent evapotranspiration by water-storage changes through root-water uptake and evaporation (shallow soil), with total ET the sum of the two ($ET_T = ET_S + ET_D$); and *Deep_drainage* accounts for drainage from the shallow into the deeper soil compartments. Adding these two soil-water-storage terms and defining a *Loss* term as the sum of three unmeasured terms, $ET_S + ET_D + \Delta S_D$, yields:

$$Loss = Rain + Snowmelt - Streamflow - \Delta S_S \quad [2]$$

Precipitation was measured at the upper and lower met stations and the average daily values from the two stations used in this analysis. *Snow* was estimated from the average of the 27 snow-depth sensors, for days showing an increase in snow depth, with the measured snow depth converted to SWE using snow-density values calculated from the co-located snow pillow and depth sensor at UM. Because the precipitation gauges are imperfect at capturing snowfall, increases measured by the snow-depth sensors were compared on a storm-by-storm basis with the gauge records. For only one event in WY 2009 did the snow-depth sensors show significantly more snowfall than was recorded by the gauges, and for this event the gauge record was corrected using the increase in SWE from the 27 snow-depth sensors. Otherwise, the match between the snow sensors and the precipitation gauge was good on a storm-by-storm basis, which is consistent with an earlier report that undercatch of snow in the rain gauges in the study area was small (Hunsaker et al (in review)). However, these two records showed differences in the day-to-day timing of snowfall. We used the precipitation gauge data to indicate the timing of precipitation, and assigned the precipitation to *Snow* on days when the average of the 27 snow-

depth sensors showed an increase, and to *Rain* when they showed no increase. We also compared the precipitation records to those from two RAWS stations (Dinkey and Shaver) in the region (<http://www.raws.dri.edu>); records showed good consistency. Corrections to the *Rain* and *Snow* terms for canopy interception and snow sublimation are discussed below. For days without snowfall, *Snowmelt* was calculated from the average of the 27 snow-depth sensors, for days showing decreases in snow depth, converted to SWE as noted above. *Streamflow* was available from the P301 and P303 stream gauges, and ΔS_s was calculated from the 27 soil-water nodes.

Results

Soil physical properties. Most sampled soils represented sandy and loamy-sand textural classes, with a sand fraction averaging 0.70 and 0.84 at LM and UM sites, respectively (Figure 2a). Soil samples were very loose, single grained (a structureless condition) and massive at depths greater than 60 cm. Dry-bulk-density values were extremely low in near-surface horizons as a result of high organic matter, about 1.0 g cm^{-3} (15 cm sampling depth). Values increased to 1.25-1.35 g cm^{-3} at 30-cm depth and to about 1.35-1.45 g cm^{-3} at 60- and 90-cm depths. There was little variation in K_s values (16 samples), 1 to 21 cm hr^{-1} , and no consistent variation with depth. However, two near-surface soil depths were higher in porosity, average K_s value of 8 cm hr^{-1} , while the two deeper sampling depths in the same profile characterized by lower porosity and K_s values averaging 3.5 cm hr^{-1} . We attributed part of the K_s variability to differences in gravel content and roots among samples, contributing to macropore flow and occasional high saturated-conductivity values.

Except for gravel content, soil textural variations are relatively small, and the spatial distribution of soil texture surprisingly uniform. Gravel and sand content increased with elevation and soil depth (Figure 2a), corresponding to a decrease in silt and clay content. There were no significant differences in texture between north- and south-facing nodes at either elevation (Figure 2b). Gravel content and both coarse and total sand fractions were larger at the higher- versus lower-elevation nodes. We attribute these findings to the control of elevation on soil formation and solum thickness, where chemical weathering rates are dampened by cooler temperatures at higher elevations. Combining all sampling depths and nodes, and computing average soil texture for the upper and lower met sites, differences in total gravel fraction (mean \pm

standard deviation) were 0.30 ± 0.13 and 0.16 ± 0.07 , respectively, with corresponding values for total sand of 0.79 ± 0.05 and 0.68 ± 0.06 , and clay of 0.06 ± 0.02 and 0.11 ± 0.04 , respectively.

Soil-landscape relationships. Entisols and Inceptisols are the only soil orders mapped in the basin. These soils are weakly developed, primarily because they occur on young landscapes. Cool climate, steep terrain and resistance of parent material to chemical weathering also limits pedogenesis in this setting. Elevation is the main factor associated with differences in soil across the basin.

The lower extent of the last glacial-ice advance occurs at an elevation of 1800 m, and as a result, soil landscapes above this elevation tend to have highly variable thicknesses with a greater expanse of rock outcrop. Scouring by glacial ice has resulted in a hard-bedrock contact in most soils, usually present within a 100-cm depth. There are three main soil families mapped in the basin, with Gerle and Cagwin found at higher elevations (1800-2400 m) and Shaver occurring at 1750-1900 m. Gerle and Cagwin have a frigid soil-temperature regime with mean annual soil temperature $< 8^{\circ}\text{C}$ and relatively warm summer temperatures, with difference between mean summer and mean winter temperatures $> 6^{\circ}\text{C}$ (Soil Survey Staff, 2010). Cagwin and Gerle families are classified as Dystric Xeropsamments and Humic Dystroxerepts, respectively. Cagwin tends to occur on erosive landscapes such as convex ridge tops, steep mountain slopes and sparsely vegetated areas intermixed with rock outcrops. As a result Cagwin is sandy, with shallow and moderately deep phases and minimal horizon differentiation (A-C horizon sequence). The Gerle family soils have an A-Bw-BC-Cr horizon sequence displaying some initial stages of pedogenesis, such as the development of soil structure, thickening of A horizons and a slight accumulation of secondary iron oxides indicated by the high chroma (≥ 4) in the subsoil (Table 1). These coarse-loamy soils have slightly finer textures than Cagwin and tend to occur on landforms with greater contributing area such as concave or linear hillslopes and sites more resistant to erosion. Soil texture of the solum was gravelly loamy coarse sands and gravelly coarse sandy loams, with average coarse fragments of 0.17-0.33 by mass (Table 1; Figure 2b). Soils in this portion of the basin have weak subangular blocky structure or structureless conditions (massive and single grained) with common to few roots below 15 cm (Table 1).

Soils of the Shaver family are in a soil landscape interpreted to be below the extent of late Pleistocene glaciation (Giger and Schmitt 1993). As a result, the bedrock is more highly

weathered and consists of unconsolidated deep regolith (saprolite) where hard bedrock is not typically encountered within a 150-cm depth. The Shaver family has a mesic soil temperature regime with mean annual soil temperature between 8 and 15°C (Soil Survey Staff, 2010). Soils of the Shaver family are classified as Pachic Humixerepts, and are finer-textured soils, gravelly, coarse sandy loams, with coarse fragments of 0.11-0.17 (Table 1; Figure 2b). Soils have a moderate subangular blocky structure and many roots throughout the solum and few to common roots in C and Cr horizons. The soils of the lower portion of the basin are typically on landforms that accumulate water and sediment, and as a result, they have thicker A horizons showing greater accumulation of litter and soil organic carbon (Table 1). These soils also have higher clay content as a result of warmer temperatures (higher chemical weathering) and more-continuous flushing of the profile with water due to a greater fraction of total precipitation as rain and more frequent snowmelt.

Soil depth. A soil-depth model was built using terrain attributes to estimate general trends in soil depth across the basin (Figure 3). Soil thickness can vary from less than 50 cm to over 150 cm across short distances (<10 m). The resulting model accounted for 16% of the variance in soil depth (adjusted R^2), and predictions were characterized by a root-mean square error of 30 cm. The relatively poor fit of the model is a result of high degree of variability in soil depth over short distances, particularly in upper parts of the basin; however, the model explains general trends in soil depth at the catchment-scale, arguably better than that of the order-four soil survey inventory. The steepest slopes, in the middle of the basin, have shallow soils (< 50 cm), low tree density, and a high frequency of rock outcrops. Similarly, soils were shallow in the upper portions of the basin, where rock outcrops were expansive. More-gently sloping terrain in the upper and lower portions of the basin with linear or convex hillslopes tended to be moderately deep (50-80 cm). Concave landforms with high tree density at the upper and lower portions of the basin support the deepest soils. When comparing the three sub-catchments, the area-average depth to bedrock for P303 is likely to be significantly larger than for the P301 and P304 sub-catchments, especially realizing that soil-depth measurements were limited to 100 cm, thus our model does not reflect the true depth of soil in areas mapped as 100 cm and these soils are potentially much deeper. We expect that depth-to-bedrock differences have a major impact on water storage and tree-available water, as well as streamflow.

Snowpack depth. Snow depths reached an average peak of about 100 cm in both water year (WY) 2008 and 2009, with peaks at individual sensors of 50-200 cm in 2008 and 70-160 cm in 2009 (Figure 4). We note that the 2008 WY starts October 1 of 2007, so that water-year day (WYD) 120 corresponds with February 1, 2008. There were two main snow events each year, occurring at the end of February 2008, and mid February 2009. There was also a rain event in January 2009, which occurred between the December and February snowstorms in WY 2009 and a smaller late mixed rain/snow event in March 2009 (Figure 4a). During the month-long warm period and rain-on-snow event in January-February 2009 snow was depleted at many sites. The two heavy snowfalls in WY 2008 resulted in greater snow-depth variability than from the smaller snow events in 2009. Snowmelt timing was also more variable in 2008 than in 2009. From the peak, snow was depleted over a 75-day period in both 2008 (WYD 150-225) and 2009 (WYD 140-215). Rates of snow depletion in January-February were generally slower at open versus under-canopy sensors, with rates comparable between sensors in March-April.

Snow depths were on average 35-40 cm greater in the open versus at the drip edge, and 45-55 cm deeper in the open versus under the canopy (Figure 5a). Differences in snow depth between under canopy versus drip edge were less significant, with snow 10-20 cm deeper at the drip edge versus under the canopy during the winter and early spring. Snow was also generally deeper at sensors in the higher versus lower elevation nodes, especially the sensors in the open (Figure 5b). Differences between snow depths on north- versus south-facing slopes were less consistent (Figure 5c).

Peak snow depth in WY 2008 occurred at the end of February; three weeks later over 1/3 of the snow had melted and LS was nearly snow free (Figure 4b). Snow persisted for approximately two weeks longer at UN. Peak snow depth in WY 2009 occurred in mid-February, four weeks earlier than in 2008. Average peak snow depth was 39 cm deeper in WY 2008 than 2009 at the upper nodes. However, average peak snow depth at the lower elevation nodes were about the same between WY 2008 and 2009. Many locations had two complete snowpack melt cycles in WY 2009, where the snowpack was persistent throughout the winter in 2008. The snowpack was completely melted at the upper sites by early May in WY 2009, approximately four weeks earlier than 2008.

Snow density, used to calculate SWE from snow-depth measurements, increased as snow consolidated and melted through the winter and spring, with drops in both years corresponding to

snowfall events (Figure 6). Note that snow density was higher in WY 2008, because of earlier and more dense snowfall events.

Soil moisture. VWC values from five of the 27 vertical profiles illustrate typical soil-moisture patterns and the wide spatial variability observed (Figure 7). Data in the first part of WY 2008 are incomplete; as logging of data from some sensors started after October 1 and some sensors needed several weeks time to ensure good contact of the sensor prongs with the surrounding soils. Despite the wide spatial variation between sensors, seasonal cycles in soil moisture were very similar across nodes and years. Peaks in spring and fall generally coincided with occasional rainfall events, with sensor response typically attenuated at deeper soil depths (e.g. October, WY 2009). Maximum VWC generally occurred in the winter, with fluctuations corresponding with snowmelt, followed by soil drainage. The coarseness of the soils resulted in rapid drainage and quick VWC responses. From the decreasing VWC values immediately after snowmelt events, one can infer typical soil field-capacity values in the range of $0.2\text{--}0.25\text{ cm}^3\text{ cm}^{-3}$ for the 60- and 90-cm soil depths. Typically, the near-surface sensors recorded the highest VWC values in wet periods, but were the driest in the summer and fall as soils became desiccated by root-water uptake and soil evaporation (e.g. UNop, Figure 7). At some instrument locations, sensors at the 10-cm depth showed VWC values that were lower than at the 30-cm depth during soil-wetting events, and VWC could be near zero in the summer and fall (e.g. UNcd-de, Figure 7). For those locations, the soil-moisture sensor was installed just below the litter layer as opposed to mineral soil and sensor contact with the surrounding material may be inadequate; the corresponding very high porosity would prevent high VWC, even during snowmelt.

The widest range in VWC within a profile occurred at sites where depth to bedrock was near 1 m or shallower. In those cases, the fraction of gravel was larger than 0.25, with some values close to 0.45-0.50. For example, gravel-content values for the UNcd-de site were between 0.35 and 0.42 for 60- and 90-cm depths, respectively. For USqk-de and UFop, field notes indicated that depth to bedrock was highly variable, ranging between 70 and 120 cm, thus precluding sensor installation at the 90-cm depth. Across most sensor profiles, the deeper sensors recorded lower VWC values than did those near the soil surface throughout the winter and spring, because of greater coarseness of the soil texture with increasing soil depth. This resulted in correspondingly lower soil-water retention. In addition, at some locations, porosities were

relatively low because sensors were placed in saprolite, thus limiting VWC values during snowmelt or rainfall periods to near $0.2 \text{ cm}^3 \text{ cm}^{-3}$ (e.g. UNcd-de and UFop).

Integrating the VWC measurements over depth to calculate total soil-moisture storage allows for an analysis of trends in soil water available for root-water uptake. Soil-moisture storage showed a clear increase in response to late-fall rain, winter snowmelt and early spring rain plus snowmelt (Figure 8a). These events were followed by a rapid and immediate decrease in soil-moisture storage, owing to rapid initial drainage in these coarse soils. Subsequent decreases in soil-moisture storage through the summer and fall provide information on root-water-uptake and transpiration rates. Sums for 0-75 cm soil depths are shown here, as not all profiles had a 90-cm VWC sensor. VWC did not show any distinct pattern with location relative to tree canopy (Figure 8b), indicating little or no canopy effects on water infiltration or soil evaporation, and a uniform lateral distribution of root-water uptake, irrespective of position within the local landscape. However, our results clearly showed that the more-well-developed soils in lower parts of the basin hold significantly more water compared to weakly developed soils in the upper reaches of the basin (Figure 8c). Average differences in soil-water storage between upper and lower met locations were about 5 cm in the winter and spring, and decreased to about 2 cm during the summer and fall as total soil-water storage decreased.

Winter soil temperatures at the lower sites were generally 0.35°C warmer than upper-elevation soils, for both north and south aspects, but there were no clear differences in spring and summer (data not shown). Soil temperature did not drop below 0°C at any location in WYs 2008 or 09. During winter of WY 2009, soils from the north-aspect sites were approximately 1.2°C colder than soils from south-aspect sites for both upper and lower elevations.

Water balance. Daily values of total precipitation and SWE (Figure 9a) and snowmelt rates, streamflow and soil-moisture storage (Figure 9b) show similar patterns in both years; these are estimated basin-wide values, based on data from Figures 5, 6 and 8, plus discharge. Cumulative snowmelt, total precipitation and stream discharge on Figure 9c use the daily data of Figures 9a and 9b. Finally, in Figure 9d, we present cumulative values of the *Loss* term, defined in Equation [2]. Note that the total WY sum of *Loss* and *Streamflow* is about equal to total *Rain* and *Snowmelt*, as the annual change in soil-water storage is near zero. There was a small change in storage for the WY 2008 data, which covers only 9.5 months.

Discussion

Soil characterization. Although there is striking uniformity in physical and morphological properties of soils throughout the basin, differences in soil depth, especially depth to hard-bedrock contact, are significant and affect soil-moisture storage and streamflow. The deeper average depth to bedrock for P303 than for the other sub-catchments result in values of annual streamflow that are only 50-75% of those for P301 (Figure 9c). The nature of the bedrock contact also affects hydrologic flowpaths such as deep percolation in the more-weathered lower-elevation soil profiles versus subsurface lateral flow over hard bedrock in glaciated terrains. Although the intensity of the soil survey (Giger and Schmitt 1993) was not sufficiently rigorous to accurately portray the spatial patterns of soil depth at the catchment-scale, the current field data, depth model and soil survey do point to significant variability within and between sub-catchments. Consistent with this finding of deeper soil in P303, using end-member-mixing analysis, Liu et al. (submitted) found near-surface runoff to contribute about 65% and 45% of annual streamflow in P301 and P303, respectively, with baseflow contributing 32% and 52%, respectively. Rainstorm runoff accounted for 3% in each.

Soil data collected in this study were limited to the 90-cm soil depth. More-recent soil sampling and excavation near the CZT-1 area indicated soil within the upper 60 cm grading to a thick zone of weathered bedrock that changed with depth from moderately dense saprolite to consolidated saprock and hard bedrock contact at 150 cm. Tree roots were uniformly distributed within soil to a depth of 60 cm. Root density significantly decreased below that depth and roots appeared to be absent below the hard bedrock contact at 150 cm. These observations also indicated high-density, low-porosity saprolite in the transition zone towards the saprock and bedrock below. Recent work by Rossi and Graham (2010) from the eastern Sierra Nevada showed porosity values of about 0.15 or less, depending on the degree of weathering of medium-grained (1-5 mm grain diameter) granitic saprolite. We observed consolidated but weathered saprock below the saprolite, containing no clay minerals and featuring the original rock fabric. The combination of porosity and the root-restrictive condition of saprolite and saprock may be an important feature in these soils that regulates streamflow during summer months. The weathered bedrock restricts access by tree roots, limiting losses from ET, and depending on its thickness across the catchment, has the storage capacity to sustain streamflow.

Soil moisture. Differences in soil moisture between the upper- and lower-elevation nodes can largely be explained by differences in soil texture. When analyzing average differences in soil-water storage between north and south-facing aspects (Figure 8d), there were no clear patterns; but typically, the south-facing slopes hold more water when the soil is wet, with differences between north- and south-facing slopes disappearing in the dry periods. Possibly, weathering rates are higher along the south-facing aspects, resulting in finer soil materials that increased soil-water retention. For the lower-elevation nodes, profile-averaged total-sand fractions for the south- and north-facing aspects were 0.64 and 0.72, respectively. No clear differentiation in sand content could be determined from soil-textural data for the upper-elevation nodes.

In addition to sensor calibration error and variations in soil texture, various other factors caused VWC variations across the study area. During the snowmelt season there is much evidence of local runoff and run-on, causing large spatial variations in soil-water content as a result of localized snowmelt infiltration and seepage, induced by microtopography. In addition, variations in coarse-fragment content (>2 mm) and occasional presence of large macropores are likely to cause preferential subsurface flows, as observed at the upper-elevation nodes. Spatial variations in snow accumulation, snowmelt and tree-root-water uptake create additional spatial variation in VWC. Moreover, other studies have demonstrated that canopy interception and resulting tree stemflow can cause concentrated rainwater infiltration under the tree canopy, leading to large variations in soil-water content that result in bypass flow and localized regions of saturated flow along the soil-bedrock interface (Liang et al., 2007).

Late-summer VWC at all depths and locations approached low values of about $0.1 \text{ cm}^3 \text{ cm}^{-3}$, indicating that both streamflow and root-water uptake depend on deeper soil storage. Soil-moisture profiles showed higher near-surface than deeper soil moisture in the winter, with an inversion occurring in spring and summer to lower VWC at the near surface than at depth (Figure 7). This was apparently caused by soil evaporation and root-water uptake, as tree roots are concentrated in the 0-60 cm soil depth. Near-surface soil horizons responded more to rain than deeper depths, which is expected.

In both WYs 2008 and 2009 there was little change in average soil moisture across all locations until the snowpack was more than 50% depleted (Figure 10). By the end of the summer, soil moisture had dropped to much lower levels, with VWC averaging $0.1 \text{ cm}^3 \text{ cm}^{-3}$. A recent report for a set of 38 measurements over a 15-month period at 57 locations in a 2-ha plot

in the mountains of Idaho showed that the spatial distribution of snow was an important determinant of soil moisture, both during and after snowmelt (Williams et al. 2009). However, the soil-water storage in our watershed was greater at the lower elevations, which had less snow and earlier snowmelt, owing to the coarser soil texture at the upper elevation nodes. Similarly, the north-facing nodes had more snow, on average (Figure 5d), but the soil-water storage for the south-facing slopes was slightly higher (Figure 8d), especially for the lower-elevation nodes.

Water balance. Streamflow showed a rapid response to precipitation and snowmelt events, which is thought to be the result of large areas characterized by shallow soils with depth to bedrock less than 1 m, steep slopes, and the relatively uniform and coarse-textured soil material. For example, this rapid response of streamflow to rainfall can be seen on WYD 97 and 116 during 2008 and 2009, respectively (Figures 9a and 9b). Similarly, soil-moisture storage (Figure 10b) shows a rapid response on those days, decaying very quickly due to the coarseness and uniformity of the soil. We also note the correspondence of snowmelt with peaks in streamflow (Figure 9b).

Soil-moisture storage in the upper 1 m of soil was approximately 20 cm through the spring, until snowmelt was complete (Figure 9b). Following the depletion of snow, both the soil moisture and streamflow receded through the end of the water year. Moisture storage for 0-75 cm depth averaged about 75% of that for 0-100 cm depth at nodes with the deeper sensor. After snowmelt was complete, moisture storage per meter depth (0-100 cm depth) declined at a rate of about 0.3 cm d^{-1} on water day 244 (June 1), declined at only 0.2 cm d^{-1} by July 1, and was less than 0.05 cm d^{-1} by Sept 1 (30 days before the end of WY 2008). In WY 2009, moisture storage declined at about 0.3 cm d^{-1} on water day 274 (July 1), reduced to 0.2 cm d^{-1} by July 15, and was below 0.05 cm d^{-1} by mid August (45 days before the end of the water year). Two earlier periods of drainage in WY 2009, WYD 45-75 and 219-240, show rates of storage decline exceeding 0.3 cm d^{-1} ; and in the first of these two periods the rate of storage decline dropped to under 0.05 cm d^{-1} 30 days later. Assuming that the declines are ET, these rates are surprisingly low for the healthy and fast-growing forest, and further suggest that tree roots are likely accessing large volumes of soil water below 1 m.

As is apparent from the cumulative precipitation and stream-discharge values (Figure 9c), only 10-15% of the precipitation in P303 and 18-19% of that in P301 left the basin as stream discharge in WY 2008 and 2009. These same differences were apparent during four earlier

water years, with water yields from adjacent P301 and P304 headwater basins 50-100% higher than P303; however, the timing of runoff across all three headwater basins was similar (Hunsaker et al. (in review)). The annual *Loss* estimates averaged 105 cm for WY 2009 and are approximately 111 for P303 and 99 cm for P301. Assuming no change in ΔS_D , this loss term includes soil evaporation, canopy interception, and transpiration. Though we did not measure canopy interception, the *Snow* estimates should not need correction as most snow-depth sensors were placed under the canopy. Assuming that canopy interception is about 20% for rainfall (Vrugt et al. 2003; Reid and Lewis 2009), which was about 59 cm, approximately 12 cm of the 105 cm *Loss* could be canopy interception. Work by Armstrong and Stidd (1967) on a water-balance study in the Sierra Nevada showed rainfall-interception losses of the same magnitude, and related to canopy density and forest cover. There could be an additional small correction for sublimation. Work by Molotch et al. (2007) reported values of 0.4-0.7 mm d⁻¹ for sites in the Rocky Mountains. However, it should be small in these forested catchments, which have low wind velocities. Thus ET was 87-99 cm, averaging about 93 cm for the two sub-catchments, with the higher value in P303 (Table 2). This 93 cm is more than four times the water storage in a 100-cm deep soil profile. Note that the change in storage of 1 cm in P301 is based on observations at CZT-1, which although qualitatively similar to that on Figure 9c, showed a small change over the year.

The role and magnitude of snowmelt storage in the basin is illustrated by the basin-wide SWE estimates (Figure 9a), and at its peak is comparable in magnitude to the maximum amount of water storage in the upper 1 m of soil. This magnitude is also important when considering the two-month time lag between cumulative precipitation and snowmelt (Figure 9c). That is, although there was snow-cover for about five months in both years, there was some snowmelt during the winter, resulting in about a two-month lag between precipitation and streamflow generated by snowmelt. The water-balance results in Figure 9d further illustrate the relatively steady flow of rain plus snowmelt delivery to the soil during snowmelt of about 0.8 cm d⁻¹ in March-April 2008 and 1 cm d⁻¹ in March-April 2009. The difference reflects the slightly later precipitation in WY 2009. Change in soil-water storage, illustrated by the difference between the lines on Figure 9d, shows the importance of this reservoir for both ET and stream discharge beginning in May of both years. The combined snowpack and soil storage effectively doubled

the amount of water available for ET, in comparison to a rain-dominated catchment with the same amount of soil storage available for ET.

To better understand the soil-water dynamics during the year, we present the average monthly and quarterly water-balance components for WY 2009 in Figure 11. The water balance for the deeper soil compartment assumes that deeper soil-water is either available storage for ET during the year, or is leaving the basin by streamflow. Therefore, the water input term is *Rain* + *Snowmelt* combined. The bar graphs clearly show the large magnitude of the *Loss* term in the winter (January-March) and early spring (April-May). However, it is expected that most of this *Loss* term corresponds with increasing deep soil-water storage that becomes available in the later spring and summer (June-August). In the late summer and early fall (September-October), the *Loss* term will tend to be near zero, as ET will largely come from the deeper soil compartment. Consequently, the deep-zone soil-water storage ($\Delta S_D < 0$) and ET ($ET_T > 0$) terms will almost cancel. Through spring and summer (May-October), the remainder of ET will come from root-water uptake in the shallow soil compartment, resulting in negative values of ΔS_D .

To further partition the loss term over the year, Figure 11c gives corrections for canopy interception of rainfall, computed by subtracting 20% of *Rain* for days with rainfall, as noted above. In order to partition the corrected loss term between ET and deep soil-water storage during the year, we used seasonal sapflow data of CZT-1, allocating the estimated ET_T to seasons in proportion to seasonal sapflow. In doing so, we estimated that WY 2009 sapflow was distributed 20% fall, 14% winter, 24% spring and 42% summer (Figure 11c). Note that a small part of the ET is soil evaporation, for which no correction was applied. The result further shows that *Loss* greatly exceeds ET_T during January through March, but that ET_T exceeds *Loss* during July-September. As $Loss = ET_T + \Delta S_D$, it appears that at least one third of the annual ET may come from the deeper storage.

Conclusions

Relatively small differences in soil texture within the study area result in significant differences in soil moisture storage across the basin. Some of these observed patterns can be attributed to differences in temperature gradients across the elevation range in the basin, while other differences in moisture storage are associated with more-local variability in soil properties. While elevation, aspect and canopy exert a strong control over snow accumulation and melt, soil

moisture showed distinct catchment-scale differences only associated with elevation differences. Thus although soil moisture variability over an area can be characterized statistically, our ability to explicitly characterize spatial patterns is limited to modeling exercises such as the depth model. Soil moisture over the basin showed a clear and spatially consistent response to snowmelt, with streamflow responding to soil-moisture storage. Soils dried out following snowmelt at relatively uniform rates; however the timing of drying at a given location may be offset by up to four weeks from another site at the same elevation owing to heterogeneity in snowmelt. Because baseflow and ET continue after soils reach a plateau of dryness, further water is apparently drawn from soil, saprolite and saprock at depths greater than 1 m.

Acknowledgements

Research was supported by the National Science Foundation, through the Southern Sierra Critical Zone Observatory (EAR-0725097) and a Major Research Instrumentation grant (EAR-0619947).

References

- Armstrong, C. F. and C. K. Stidd. 1967. A moisture balance profile on the Sierra Nevada. *J. Hydrol.* **5**: 258-268.
- Bales, R. C., M. Conklin, B. Kerkz, S. Glaser, J. W. Hopmans, C. Hunsaker, M. Meadows and P. C. Hartsough. 2011 In press. Soil moisture response to snowmelt and rainfall a Sierra Nevada mixed conifer forest. *In* D. Levia, D. Carlyle-Moses and T. Tanake. (ed.) *Forest Hydrology and Biogeochemistry: Synthesis of Research and Future Directions*. Springer-Verlag, Heidelberg, Germany.
- Bales, R. C., N. P. Molotch, T. H. Painter, M. D. Dettinger, R. Rice and J. Dozier. 2006. Mountain hydrology of the western United States. *Water Resour. Res.* **42**(8): W08432.
- Band, L. E.. 1993. Effect of land surface representation on forest water and carbon budgets. *J. Hydrol.* **150**: 749-772.
- Christensen, L., C. L. Tague and J. S. Baron. 2008. Spatial patterns of simulated transpiration response to climate variability in a snow dominated mountain ecosystem. *Hydrol. Process.* **22**(18): 3576-3588.
- Faria, D. A., J. W. Pomeroy and R. L. H. Essery. 2000. Effect of covariance between ablation and snow water equivalent on depletion of snow-covered area in a forest. *Hydrol. Process.* **14**(15): 2683-2695.
- Gee, G. W. and D. Or. 2002. Particle size analysis. p. 255–293. *In* J.H. Dane and G.C. Topp (ed.) *Methods of soil analysis, Part 4, Physical methods*. SSSA, Madison, Wi..
- Gesch, D., G. Evans, J. Mauck, J. Hutchinson and W. J. Carswell Jr.. 2009. The National Map - Elevation: U.S. Geological Survey Fact Sheet 2009-3053, 4 p. from <http://ned.usgs.gov/>.
- Giger, D. R. and G. J. Schmitt. 1993. *Soil Survey of Sierra National Forest*. United States Department of Agriculture Forest Service, Soil Conservation Service.
- Green, S. R. and B. E. Clothier. 1988. Water use of kiwifruit vines and apple trees by the heat-pulse technique. *J. Exp. Bot.* **39**(1): 115-123.
- Harrell, F. E.. 2001. *Regression modeling strategies: with applications to linear models, logistic regression, and survival analysis*. New York, Springer-Verlag.
- Hunsaker, C., T. Whitaker and R. C. Bales. In review. Snowmelt runoff and water yield along elevation and temperature gradients in California's southern Sierra Nevada. *J. Am. Water Resour. As.*

- Kizito, F., C. S. Campbell, G. S. Campbell, D. R. Cobos, B. L. Teare, B. Carter and J. W. Hopmans. 2008. Frequency, electrical conductivity and temperature analysis of a low-cost capacitance soil moisture sensor. *J. Hydrol.* **352**(3-4): 367-378.
- Liang, W.-L., K. i. Kosugi and T. Mizuyama. 2007. Heterogeneous soil water dynamics around a tree growing on a steep hillslope. *Vadose Zone J.* **6**(4): 879-889.
- Liu, F., C. Hunsaker and R. C. Bales. Submitted. Controls of streamflow pathways in small catchments across the snow-rain transition in the southern Sierra Nevada, California. *Hydrol. Process.*
- Molotch, N. P. and R. C. Bales. 2005. Scaling snow observations from the point to the grid element: implications for observation network design. *Water Resour. Res.* **41**.
- Molotch, N. P., P. D. Blanken, A. A. Williams, R. K. Turnipseed, R. K. Monson and S. A. Margulis. 2007. Estimating sublimation of intercepted and sub-canopy snow using eddy covariance systems. *Hydrol. Process.* **21**: 1567-1575.
- Molotch, N. P., P. D. Brooks, S. P. Burns, M. Litvak, R. K. Monson, J. R. McConnell and K. Musselman. 2009. Ecohydrological controls on snowmelt partitioning in mixed-conifer sub-alpine forests. *Ecohydrology* **2**(2): 129-142.
- Musselman, K. N., N. P. Molotch and P. D. Brooks. 2008. Effects of vegetation on snow accumulation and ablation in a mid-latitude sub-alpine forest. *Hydrol. Process.* **22**(15): 2767-2776.
- Reid, L. M. and J. Lewis. 2009. Rates, time, and mechanisms of rainfall interception loss in a coastal redwood forest. *J. Hydrol.* **375**: 359-470.
- Reynolds, W. D. and D. E. Elrick. 2002. Constant head soil core (tank) method. Madison, Wisconsin, Soil Science Society of America.
- Rice, R. and R. C. Bales. 2010. Embedded-sensor network design for snow cover measurements around snow pillow and snow course sites in the Sierra Nevada of California. *Water Resour. Res.* **46**(3): WO3537.
- Robinson, D. A., C. S. Campbell, J. W. Hopmans, B. K. Hornbuckle, S. B. Jones, R. Knight, F. Ogden, J. Selker and O. Wendroth. 2008. Soil moisture measurement for ecological and hydrological watershed-scale observatories: A review. *Vadose Zone J.* **7**(1): 358-389.
- Rossi, A. M. and R. C. Graham. 2010. Weathering and porosity formation in subsoil granitic clasts, Bishop Creek moraines, California. *Soil Sci. Soc. Am. J.* **74**(1): 172-185.

- Soil Survey Staff. 2010. Keys to Soil Taxonomy. Washington DC, United States Department of Agriculture, Natural Resources Conservation Service.
- Topp, G. C., J. L. Davis and A. P. Annan. 1980. Electromagnetic determination of soil water content: Measurements in coaxial transmission lines. *Water Resour. Res.* **16**(3): 574-582.
- Van Mantgem, P. J., N. L. Stephenson and J. E. Keeley. 2006. Forest reproduction along a climatic gradient in the Sierra Nevada, California. *Forest Ecol. Manag.* **225**(1-3): 391-399.
- Vereecken, H., J. A. Huisman, H. Bogaert, J. Vanderborght, J. A. Vrugt and J. W. Hopmans. 2008. On the value of soil moisture measurements in vadose zone hydrology: A review. *Water Resour. Res.* **44**: W00D06.
- Vrugt, J. A., S. C. Dekker and W. Bouten. 2003. Identification of rainfall interception model parameters from measurements of throughfall and forest canopy storage. *Water Resour. Res.* **39**(9): 1251.
- Williams, C. J., J. P. McNamara and D. G. Chandler. 2009. Controls on the temporal and spatial variability of soil moisture in a mountainous landscape: the signature of snow and complex terrain. *Hydrol. Earth Syst. Sc.* **13**(7): 1325-1336.

Table 1. Morphologic characteristics of dominant soils^a

Type	Horizon	Depth, cm	Boundary ^b	Color (dry)	Texture class ^c	CF ^d , %	Structure ^e	Roots ^f
Gerle	Coarse-loamy, mixed, frigid Humic Dystroxerepts							
	Oe	2.5-0	-	-	-	-	-	-
	A1	0-8	CS	10YR 5/3	GRCOSL	29	1FSBK	2F&M; 1CO
	A2	8-18	GS	10YR 5/2	GRCOSL	27	1FSBK	2CO
	A3	18-36	CW	10YR 5/3	GRCOSL	31	1FSBK	1 CO
	Bw	36-66	GW	10YR 6/4	GRLOCS	20	1FSBK	1 CO
	BC	66-97	GW	10YR 6/3	GRLOCS	33	MA	1M
	Cr	97-105	CW	10YR 7/3	COS	-	-	1 M
	R	105+	-	-	-	-	-	-
Cagwin	Mixed, frigid Dystric Xeropsamments							
	Oe	1-0	-	-	-	-	-	-
	A1	0-13	AW	10YR 4/1	GRLOCS	25	SG	3 VF&F
	C1	13-43	GS	10YR 6/4	GRLOCS	17	SG	2 F&M; 1CO
	C2	43-81	AW	10YR 7/4	GRLOCS	20	SG	2 M; 1CO
	Cr	81-90	AW	10YR 8/1	COS	-	-	1M&CO
	R	90+	-	-	-	-	-	-
Shaver	Coarse-loamy, mixed, mesic Pachic Humixerept							
	Oi	7.5-5	-	-	-	-	-	-
	Oa	5-0	AS	-	-	-	-	-
	A1	0-5	CW	10YR 4/2	GRCOSL	17	2FSBK	3F; 2M; 1CO
	A2	5-12	CW	10YR 5/2	COSL	13	2FSBK	3F; 2M; 1CO
	A3	12-84	AW	10YR 5/3	COSL	14	1FSBK	3F; 2M; 1CO
	C	84-185	AI	10YR 6/3	COSL	11	MA	2F&CO
	Cr	185+	-	-	COS	-	-	1CO

^a Characteristics assembled from field observations, laboratory analysis, and soil survey report (Giger and Schmitt, 1993).

^b CS: clear smooth, GS: gradual smooth, GW: gradual wavy, CW: clear wavy, AW: abrupt wavy, AS: abrupt smooth, AI: abrupt irregular

^c GRCOSL: gravely coarse sandy loam, GRLOCS: gravely loamy coarse sand, COS: coarse sand, COSL: coarse sandy loam

^d Coarse fragments >2mm and <76 mm

^e 1: weak, 2: moderate; F: fine; SBK: subangular blocky, MA: massive, SG: single grained

^f 1: few (>1 per area), 2: common (1 to >5 per area), 3: many >5 per area); VF:>1 mm, F: fine (1 to < 2 mm), M: medium (2 to < 5 mm); CO: coarse (≥5 mm)

Table 2. WY 2009 annual water balance quantities (in cm)^a

Area	Precipitation	<i>Rain</i>	<i>Snow-melt</i>	ΔS_s	<i>Stream-flow</i>	<i>Loss</i>	ET_T
P301	122	59	63	1	22	99	87
P303	122	59	63	0	11	111	99
Average	122	59	63	0	16	105	93

^aSee Equation [2]

List of Figures

1. CZO map: a) location, CZO catchments, instrument and sensor locations with 10-m elevation contours, b) upper met station and c) lower met station sensor locations with 2-m elevation contours.
2. Soil texture for: a) samples from upper and lower elevation nodes, by depth (cm); and b) average soil texture with gravel removed for nodes at the five sensor locations.
3. Soil depth to bedrock from model.
4. Temperature, precipitation and snow data for WY 2008 and 2009: a) daily average air temperature and precipitation measured in rain gauges. b) daily snow depth from 27 sensors at the five locations, with legends indicating tree species (see text), and c) mean and standard deviation of snow depths. WY 2008 record begins in February, when the sensor network became fully operational.
5. Difference in snow depth: a) mean and standard deviation of depths in the open (five sensors) minus those at the drip edge (11 sensors) or under the canopy (11 sensors), b) differences at upper minus lower elevation nodes, separated by open, drip edge and under canopy, and c) depths at sensors on north-facing vs. south-facing slopes at both elevations, with sensors in the open, at the drip edge and under canopy averaged.
6. Daily snow depth and SWE measured at upper met snow pillow for a) WY 2008, b) WY 2009, and c) snow density based on those values.
7. Vertical profiles of hourly volumetric water content measured at five vertical profiles, at 10, 30, 60, 90 cm depths. Each line is for a single sensor.
8. Daily moisture storage for WY 2008 and 2009 from 27 profiles: a) lines are means and shading is standard deviation of all profiles, b) values for open, drip edge and under canopy across all profiles, c) values for 17 upper- and 10 lower-elevation profiles, and d) values for north (UN, LN) versus south (US, LS) facing locations, and flat placement (UF).
9. Daily water balance for WY 2008 and 2009: a) daily precipitation for Providence met stations and average SWE (from Figures 4 and 6); b) streamflow for P303, daily snowmelt (based on changes in SWE in upper panel) and average moisture storage in upper 1 m of soil (average of 27 sensors); c) cumulative snowmelt, precipitation and discharge, from a and b panels; and d) cumulative fluxes into and out of catchment soils, where difference between

rain + melt and loss + discharge curves represents change in storage. Note that for WY 2008 data were only available beginning mid December.

10. Distributions of snow depth and 30-cm VWC values from 27 instrument nodes.
11. Average water-balance components for WY 2009, averaged over P301 and P303: a) average monthly and b) seasonal water-balance terms from Figure 8, and c) *Loss* term corrected for canopy interception, compared with seasonal distribution of ET based on CZT-1. Quarters are 1) OND, 2) JFM, 3) AMJ, 4) JAS.

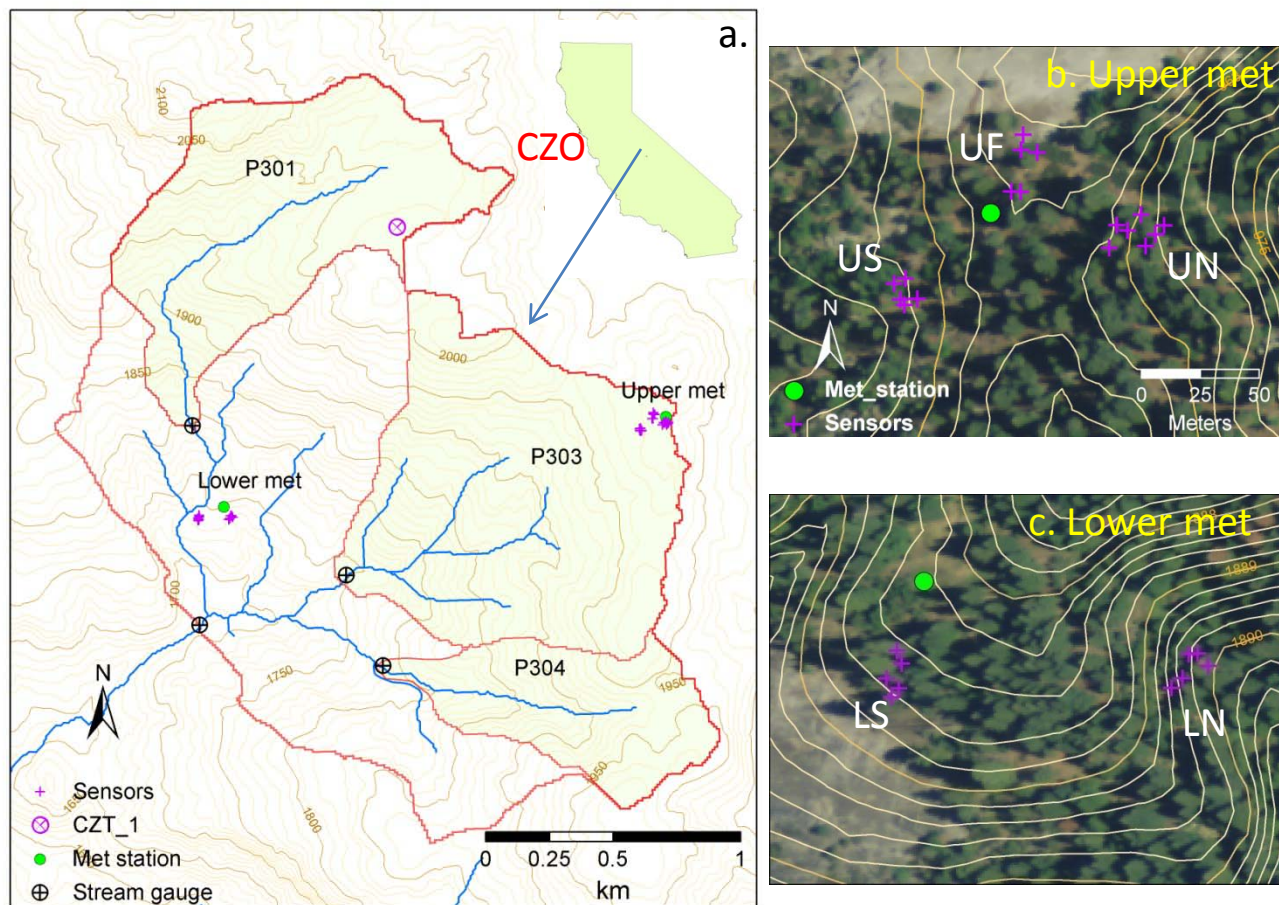


Figure 1. CZO map: a) location, CZO catchments, instrument and sensor locations with 10-m elevation contours, b) upper met station and c) lower met station sensor locations with 2-m elevation contours.

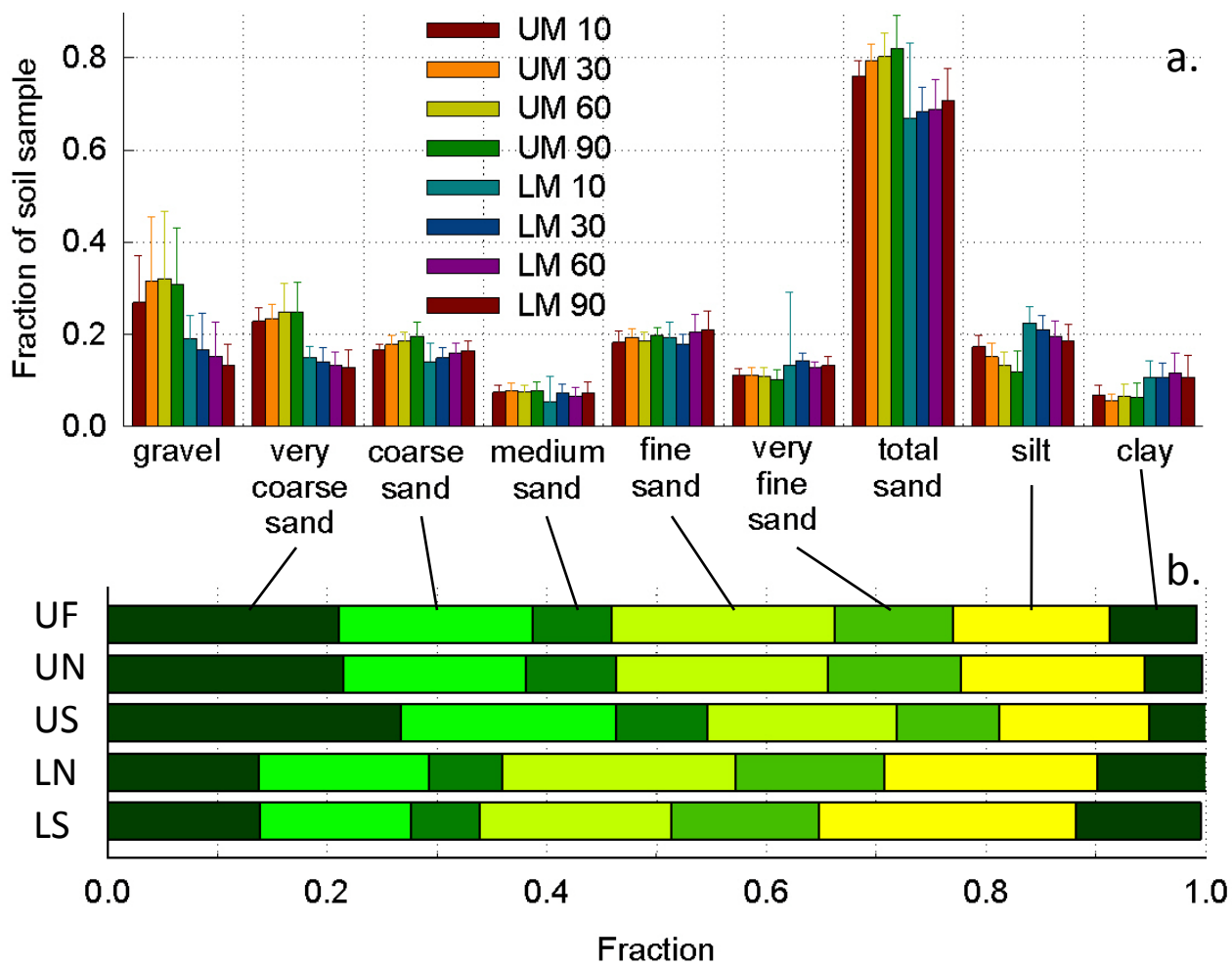


Figure 2. Soil texture for: a) samples from upper versus lower elevation nodes, by depth (cm); and b) average soil texture with gravel removed for nodes at the 5 sensor locations.

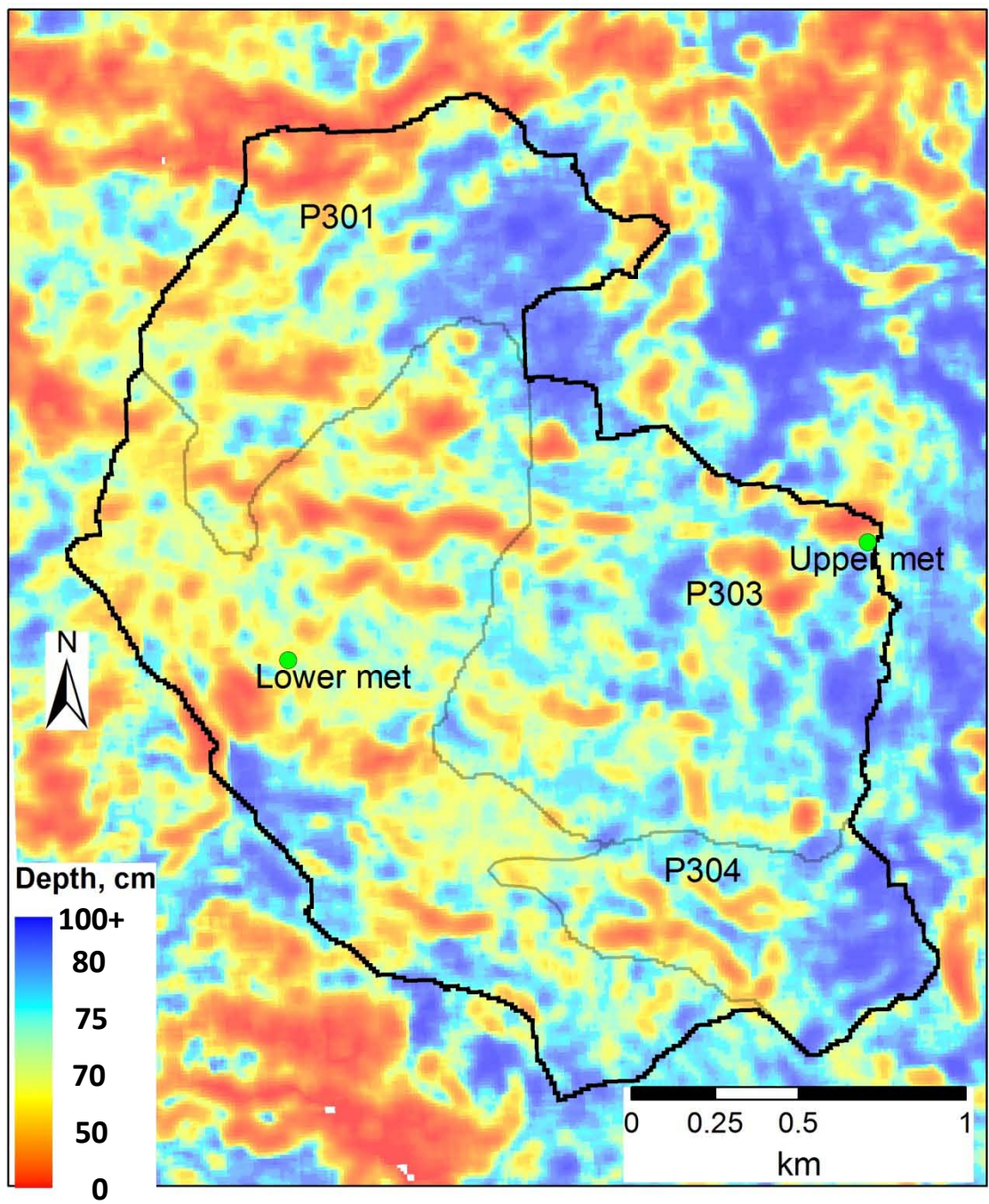


Figure 3. Soil depth to bedrock from model.

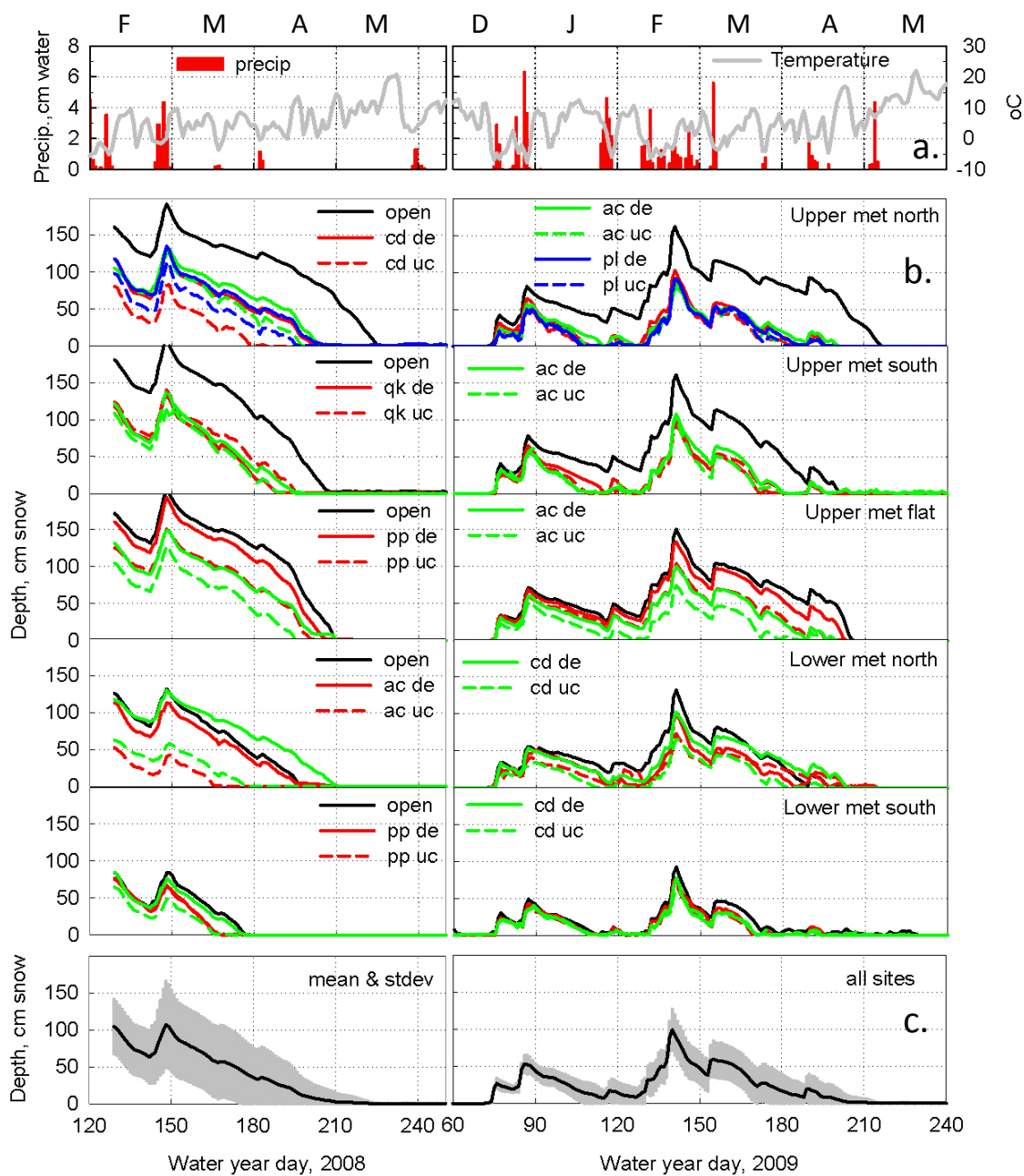


Figure 4. Temperature, precipitation and snow data for WY 2008 and 2009: a) daily average air temperature and precipitation measured in rain gauges. b) daily snow depth from 27 sensors in the 5 locations, with legends indicating tree species (see text), and c) mean and standard deviation of snow depths. WY 2008 record begins in Feb, when the sensor network became fully operational.

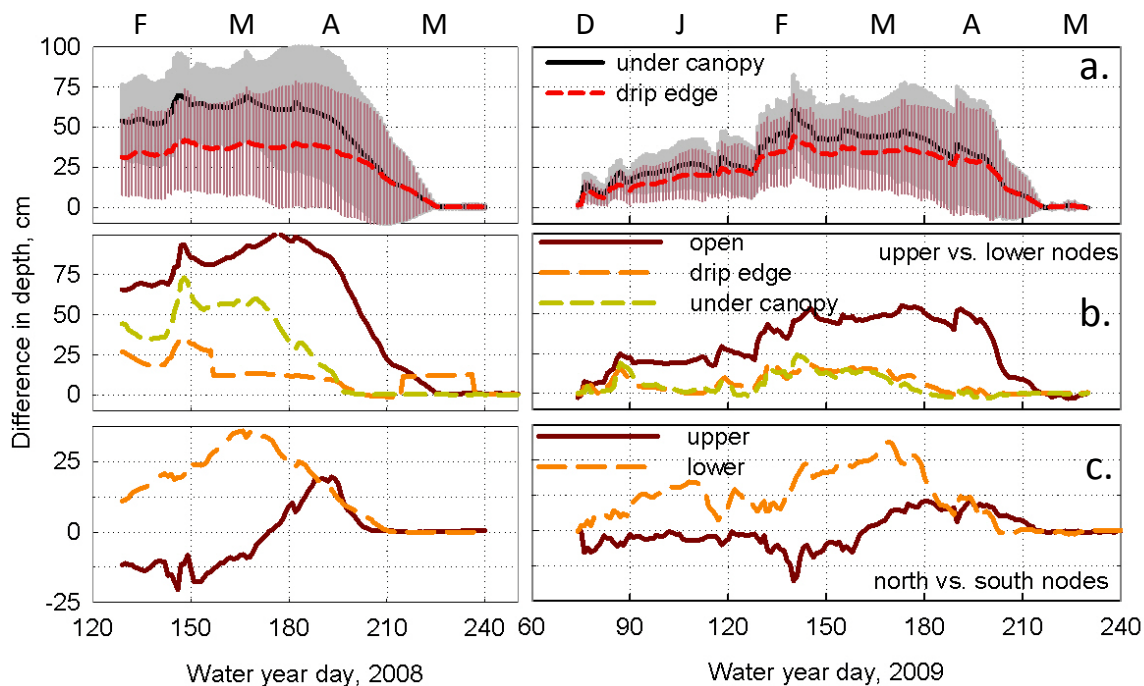


Figure 5. Difference in snow depth: a) mean and standard deviation of depths in the open (5 sensors) minus those at the drip edge (11 sensors) or under the canopy (11 sensors), b) differences at upper minus lower elevation nodes, separated by open, drip edge and under canopy, and c) depths at sensors on north-facing vs. south-facing slopes at both elevations, with sensors in the open, at the drip edge and under canopy averaged.

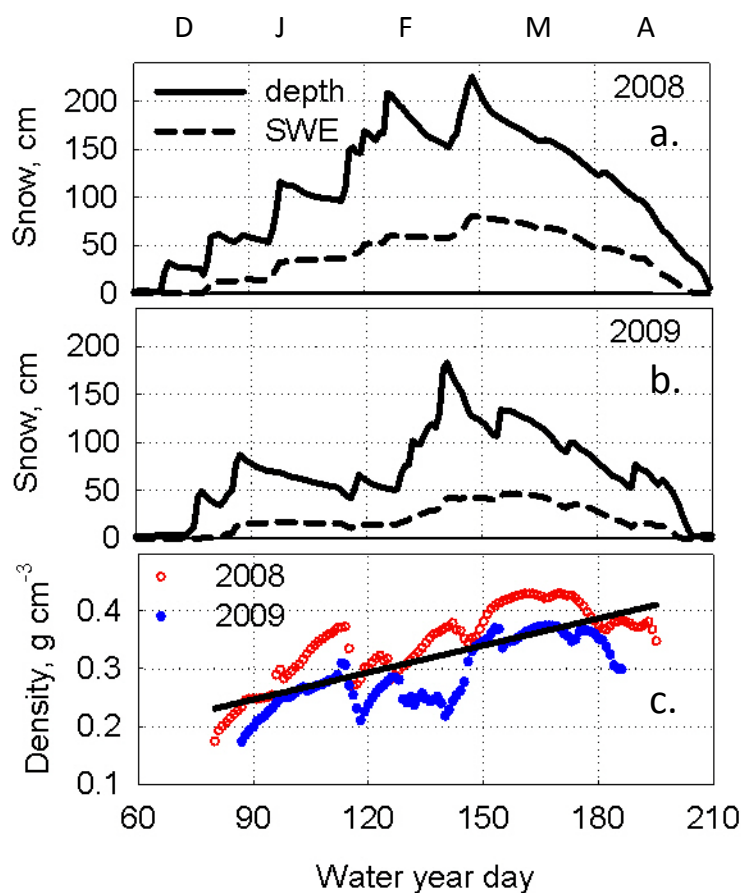


Figure 6. Daily snow depth and SWE measured at upper met snow pillow for a) WY 2008, b) WY 2009, and c) snow density based on those values.

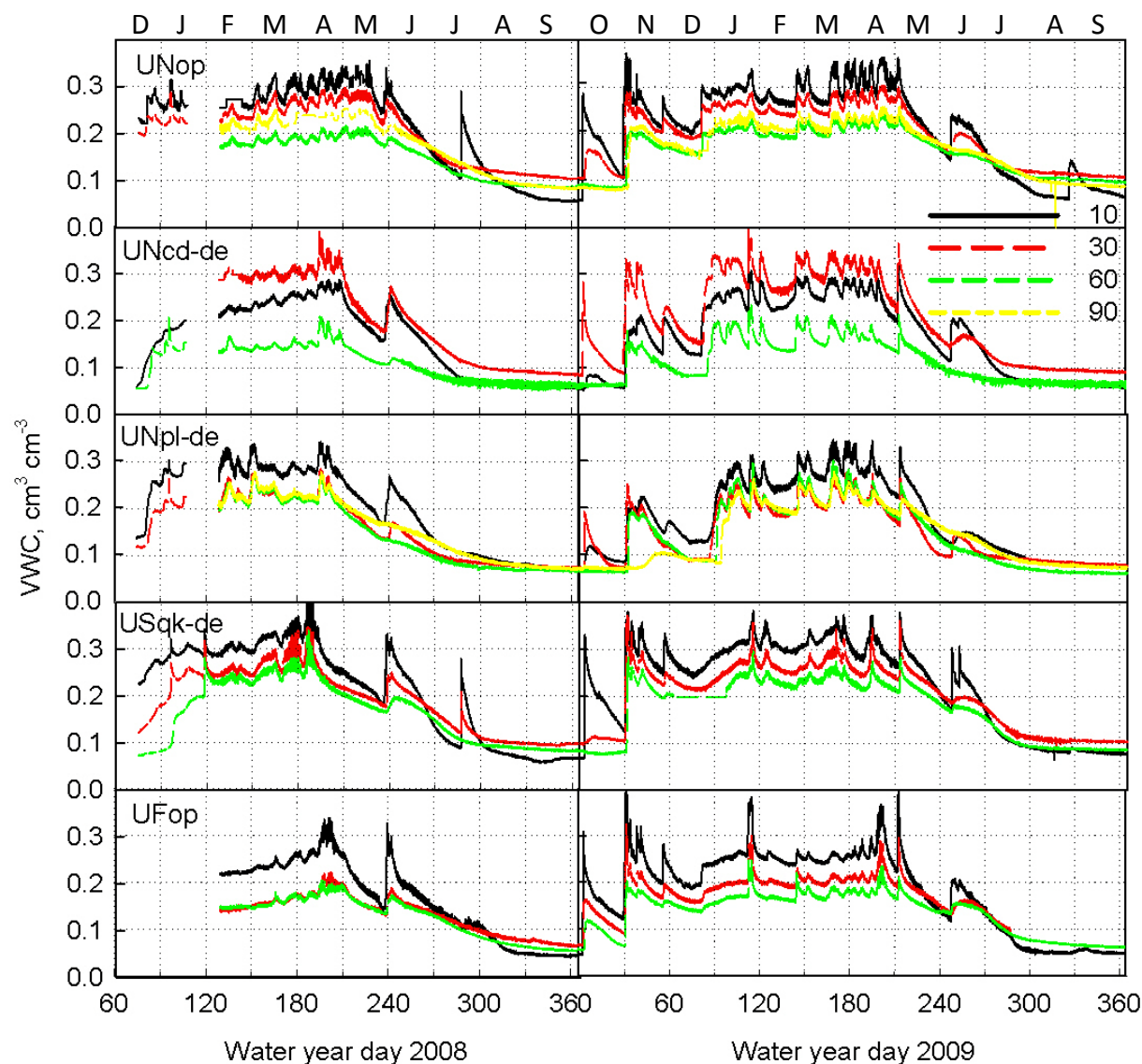


Figure 7. Vertical profiles of hourly volumetric water content measured at 5 vertical profiles, at 10, 30, 60, 90 cm depth. Each line is for a single sensor.

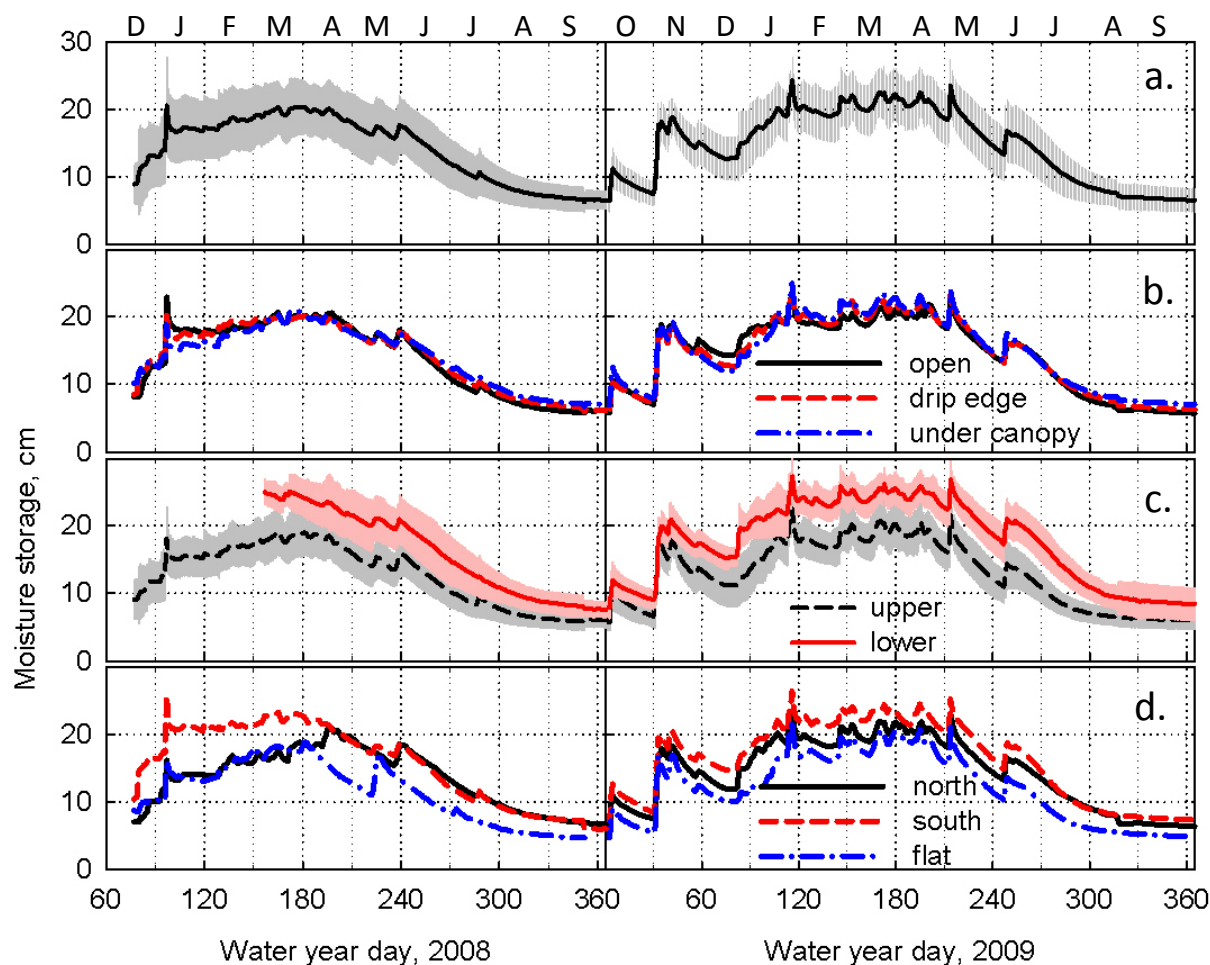


Figure 8. Daily moisture storage for water years 2008 and 2009 from 27 profiles.: a) ines are mean and shading standard deviation of all profiles, b) values for open, drip edge and under canopy across all profiles, c) values for upper 17 and lower 10 profiles, and d) values for north (UN, LN) versus south (US, LS) facing locations, and flat placement (UF).

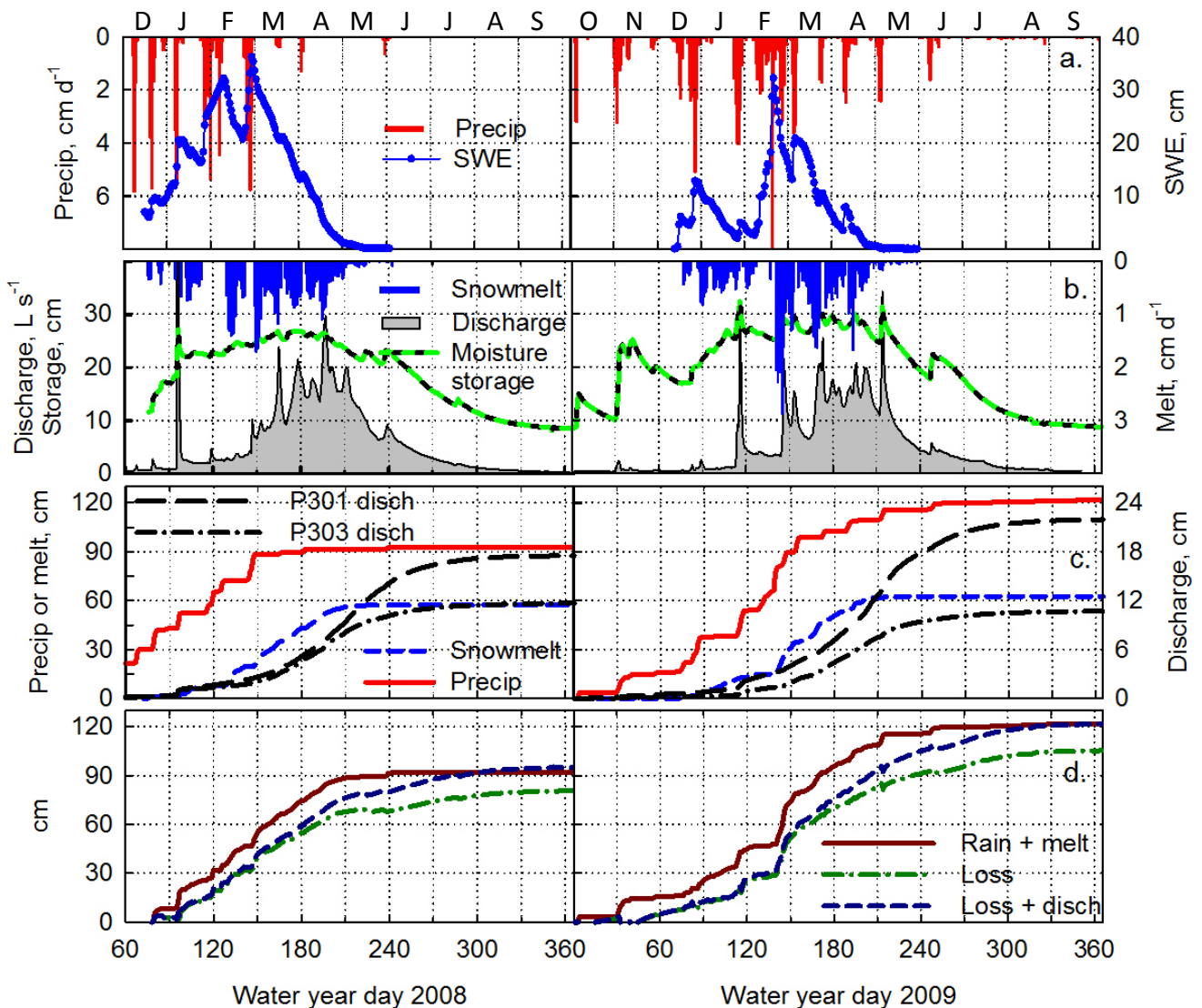


Figure 9. Daily water balance for WY 2008 and 2009: a) daily precipitation for Providence met stations and average SWE (from Figures 4 and 6); b) streamflow for P303, daily snowmelt (based on changes in SWE in upper panel) and average moisture storage in upper meter of soils (average of 27 sensors); c) cumulative snowmelt, precipitation and discharge, from a and b panels; and d) cumulative fluxes into and out of catchment soils, where difference between rain + melt and loss + discharge curves represents change in storage. Note that for WY 2008 data were only available beginning mid December.

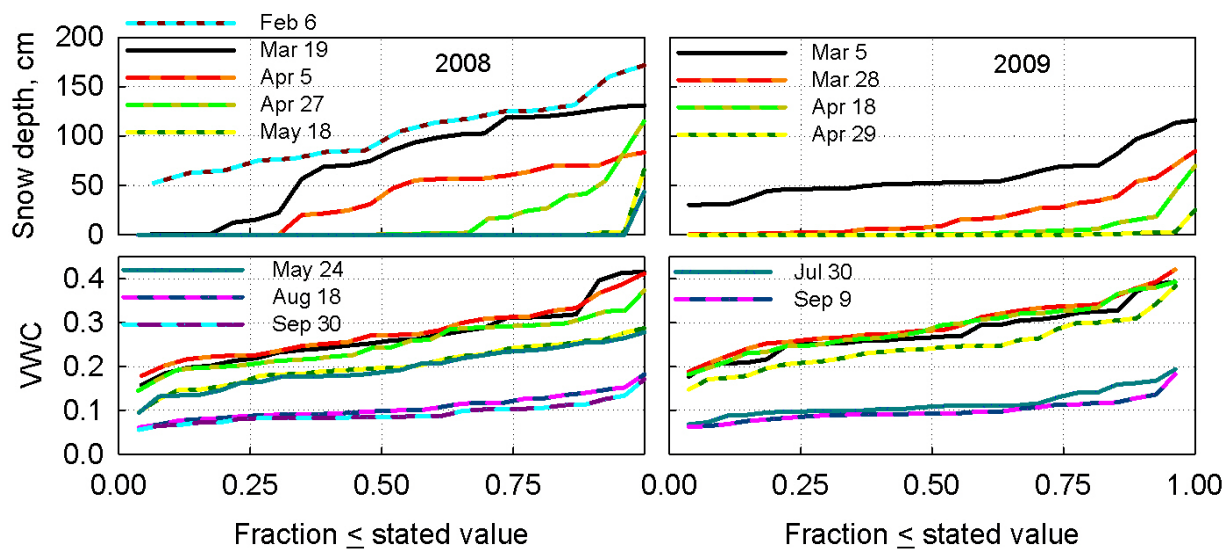


Figure 10. Distributions of snow depth and 30-cm VWC values.

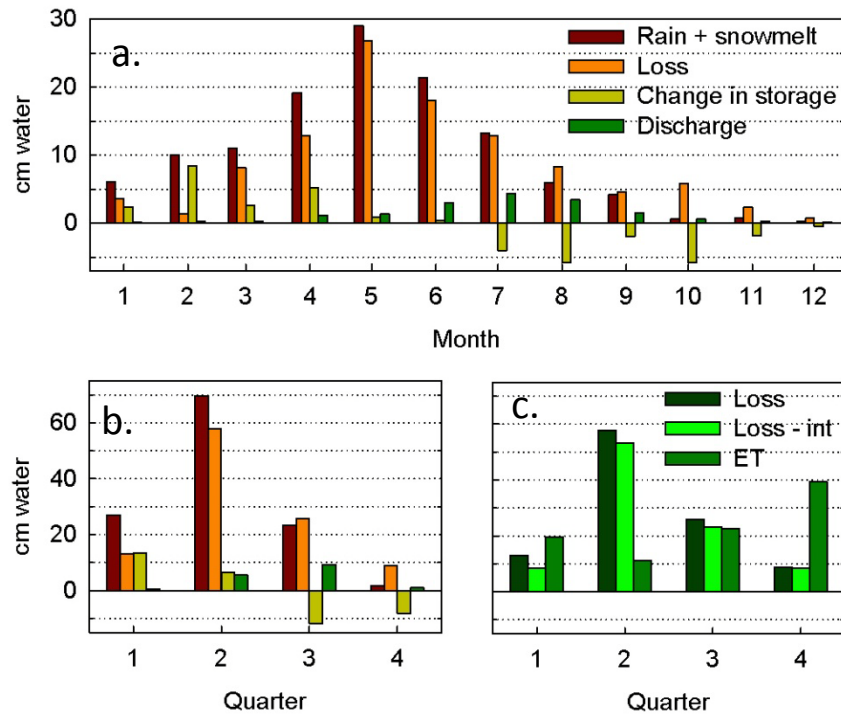


Figure 11. Average water-balance components for W Y2009, averaged over P301 and P303: a) average monthly and b) seasonal water-balance terms from Figure 9, and c) *Loss* term corrected for canopy interception, compared with seasonal distribution of ET based on CZT-1. Quarters are 1) OND, 2) JFM, 3) AMJ, 4) JAS.